Nano Communication Networks 10 (2016) 68–78

Contents lists available at ScienceDirect

Nano Communication Networks

journal homepage: www.elsevier.com/locate/nanocomnet

Graphene terahertz devices for communications applications

Mehdi Hasan, Sara Arezoomandan, Hugo Condori, Berardi Sensale-Rodriguez *

Department of Electrical and Computer Engineering, The University of Utah, Salt Lake City, UT 84112, USA

ARTICLE INFO

Article history:
Received 19 January 2016
Received in revised form
28 May 2016
Accepted 12 July 2016
Available online 28 September 2016

Keywords:
Graphene
Terahertz
Communications
Modulators
Detectors
Phase-shifting

ABSTRACT

The extraordinary electronic, thermal and optical properties of graphene, together with its two dimensional nature, and with the possibility of facile integration, have enabled its application into a new generation of high-performance devices capable of extending the performance of existing terahertz communications technologies. Although promising for wireless communications applications, the terahertz region of the spectrum, i.e. the frequency range between 300 GHz and 10 THz, is in fact still characterized by a lack of efficient, compact, solid state components capable of operating at room temperature. In this regard, graphene-based terahertz components have shown very promising results in terms of modulation, detection, as well as generation of terahertz waves. This paper will review and discuss recent progress on graphene based devices for modulation, detection and generation of terahertz waves, which are among the key components for future terahertz band communications systems.

1. Introduction

Demand for data bandwidth on wireless networks has rapidly increased over the past two decades. Edholm's law predicts that the requirement for bandwidth doubles every 18 months [1–3]. In this regard, there are two possible ways of increasing bandwidth so to satisfy this need, namely: (a) increasing the efficiency of spectral utilization, e.g. by means of using MIMO approaches and/or advanced modulation techniques, and (b) employing higher frequency carriers. Nevertheless, owed to the fact that there is an upper bound for the maximum bandwidth attainable by signal processing techniques, the need for resorting to higher carrier frequencies becomes inevitable. Based on this necessity, and also on other interesting capabilities, such as its propagation on non-metallic media, including typical building materials, the terahertz region of the spectrum has turned into a growing technological field for wireless communications applications [4,5]. However, in order to enable efficient use of terahertz carriers in practical communications links, development of different system components, such as sources, detectors, switches, modulators, filters, and amplifiers, is still a necessity. Furthermore, most conventional materials usually used at lower frequency ranges, such as the millimetre-wave and the microwave ranges, cannot efficiently respond to terahertz frequencies [6–8] and typically exhibit large loss at these frequencies. Moreover, in addition to passive materials, practical applications require electromagnetically reconfigurable materials, which constitute the basis of all active terahertz components. In this context, graphene has been recently proposed as a terahertz active material enabling multiple applications in terahertz devices.

Graphene is a two-dimensional material composed of carbon atoms arranged in a hexagonal lattice. Although its existence had been predicted by physicists long time ago, it was not until 2004 that graphene was experimentally obtained [9,10]. Early graphene synthesis resulted from the mechanical cleavage of graphite crystals using an adhesive tape. Soon after, various other techniques were developed, being Chemical Vapour Deposition (CVD) growth one of the most popular synthesis processes nowadays [11–13]. Although mechanical exfoliation can lead to excellent graphene quality in terms of mobility, defects, uniformity, and grain dimensions, the sample sizes resulting from this technique are relatively small, i.e. in the order of $<$ hundreds of microns. From this perspective, CVD graphene results more appropriate for applications requiring large area graphene, including most devices proposed to-date for terahertz communications applications. Although CVD synthesis of materials has been employed since the 1960's [10], it was not until after the first discovery graphene, by means of mechanical exfoliation, that researchers started developing and optimizing this method for the production of graphene. From this point of view, there are still many challenges, like doping control, that still need to be addressed in terms of materials processing. Nonetheless, recent progress in terms of CVD growth is remarkable. For instance, Bae et al. [13] reports on a method to grow single layer graphene in large area copper foils and the transfer of such films into arbitrary

* Corresponding author.
E-mail address: berardi.sensale@utah.edu (B. Sensale-Rodriguez).

http://dx.doi.org/10.1016/j.nancom.2016.07.011
1878-7789/

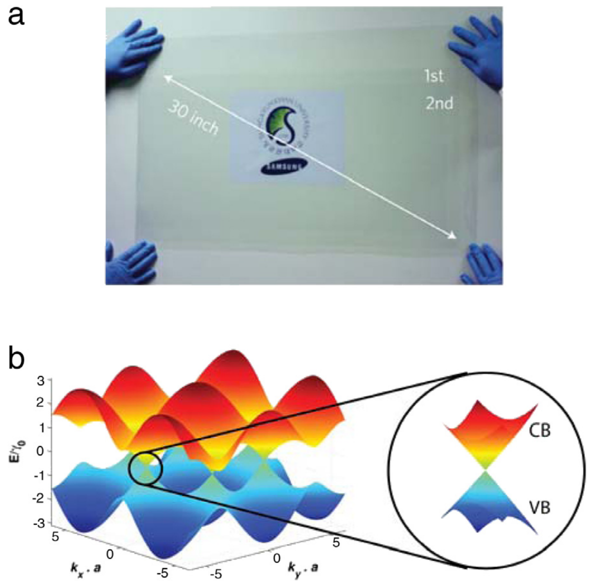

Fig. 1. (a) A transparent ultra large-area CVD graphene film transferred on a 35-inch PET sheet. Reprinted with permission from Ref. [13]. Copyright 2010 Nature Publishing Group. (b) Sketch of the band structure of graphene.

substrates, showing growth and transfer into up to 30 inch substrates as depicted in Fig. 1(a). During recent years several methods have been developed for transferring CVD graphene from the materials where is typically grown (e.g. Cu, Ni, etc.) to arbitrary host substrates, including wet and dry processes [14–19].

Graphene exhibits extraordinary properties, which are a result of its intrinsic two-dimensional nature. In contrast with typical, bulk, semiconductors, graphene holds a gapless, linear, energy vs. momentum (E–k) dispersion [20], as depicted in Fig. 1(b). Arising from this particular E–k dispersion, charge carriers in graphene behave as massless Dirac Fermions. In practice, very large mobility is possible in graphene films, e.g. mobility of up to 10^6 cm^2/Vs has been reported in suspended samples [21]. Several devices have been developed based on the electronic properties of graphene such as graphene Field Effect Transistors (FETs) and graphene inductors [22–25]. But, in addition to its remarkable electronic properties, graphene also possess very interesting optoelectronic properties, such as broadband optical absorption, which have lead into the possibility of using graphene as a material enabling applications in communication systems at various wavelengths [26–28]. Because of graphene being a gapless semiconductor, its conduction and valence bands intersect at one point, which is called the "Dirac point". Upon optical excitation, there are two possible optical transitions that can take place, namely, interband and intraband transitions. The optical conductivity of graphene can be modelled as the superposition of two independent components arising from these two types of transitions [29]:

$$\sigma(\omega) = \sigma_{intra}(\omega) + \sigma_{inter}(\omega)$$
$$= \frac{ie^2 E_f}{\pi \hbar^2 \left(\omega + \frac{i}{\tau}\right)} + \frac{ie^2\omega}{\pi} \int_0^\infty \frac{f\left(\varepsilon - E_f\right) - f\left(-\varepsilon - E_f\right)}{(2\varepsilon)^2 - (\hbar\omega - i\Gamma)^2} d\varepsilon,$$

here, e is electron charge, E_f is Fermi level, $\hbar$ is the reduced Planck constant, ω is angular frequency, τ is momentum relaxation time, $f(.)$ is the Fermi distribution function, and Γ is a coefficient that describes the broadening of interband transitions. In deriving the interband conductivity term, it is assumed that $E_f \gg k_B T$.

In the low frequency regime, intraband transitions dominate on the conductivity of graphene, since long wavelength photons do not carry enough energy to enable direct band-to-band transitions thus can mainly trigger intraband transitions. In the terahertz range, therefore, the interband contribution becomes negligible and thus the optical conductivity of graphene can be described with a Drude dispersion formula:

$$\sigma(\omega) = \frac{\sigma_{DC}}{1 + j\omega\tau},$$

in which σ_{DC} is the direct current (DC) electrical conductivity of graphene and τ is electron momentum relaxation time. By controlling the carrier concentration in graphene, its conductivity can be arbitrarily tuned. Based on this phenomena, a series of graphene-based reconfigurable devices, which can find application in future terahertz communications systems, have been proposed. In the sections to follow we will discuss recent progress in terms of such devices, namely on: graphene-based terahertz modulators (Section 2), graphene-based terahertz emitters (Section 3), and graphene-based terahertz detectors (Section 4).

2. Graphene-based terahertz modulators

2.1. Amplitude modulators

Due to its large conductivity swing, which is superior to that of other semiconductor layers, graphene has attracted lots of attention as a material for terahertz modulators [30]. Recent studies have reported large modulation depth and broadband operation in the terahertz regime by actively controlling the carrier concentration of a graphene layer and via the integration of graphene with metamaterials under different configurations [27,31–47]. In 2012, Sensale-Rodriguez et al. reported for the first time a broadband graphene terahertz electro-absorption modulator [48]. By applying a voltage between a graphene layer and a silicon substrate, in a large-area FET-like configuration, the Fermi level in the graphene film can be controlled. In those devices around 15% modulation depth was reported [48,49]. Although the modulation depth achieved using this technique is remarkable, when considering that the active material is just one atom thick, the overall device performance is still far away from what is required by system applications. However, there are several ways in which to improve modulation depth. One of these is via using reflection mode structures [50,51]. Integration of graphene into such structures can boost the absorption in graphene due to electric field enhancement when the distance between graphene and a reflector (e.g. a metallic layer coated into the back of the substrate in which graphene is transferred) is matched to an odd multiple of a quarter wavelength [50]. The device structure, which consists of a graphene layer on a silicon/silicon-dioxide substrate is depicted in Fig. 2(a). Measurements of reflectance from the structure as a function of bias voltage show that (i) at the frequency at which the substrate thickness is matched to an odd multiple of a quarter wavelength, i.e. 0.62 THz maximum reflectance modulation is attained, and (ii) $>$64% amplitude modulation with 2 dB insertion loss is possible in this structure, as shown in Fig. 2(b). However, because of the characteristics of its geometry, the response of this structure is narrow band, and owed to the large area of the device ($\sim cm^2$) the modulation speed is limited (i.e. $<$10 kHz).

Terahertz modulation is also attainable in graphene plasmonic structures. In this regard, Ju et al. proposed a design based on stripes of graphene [52]. By changing the carrier density in graphene it is possible to shift the geometric plasmonic resonance of the device thus achieve amplitude modulation. However, the extinction levels attainable in these structures at terahertz frequencies (at the plasmonic resonance) is $\sim$14%, which is limited by the maximum achievable DC conductivity in typical quality CVD graphene, and which can be enhanced by resorting to reflection mode configurations [53].

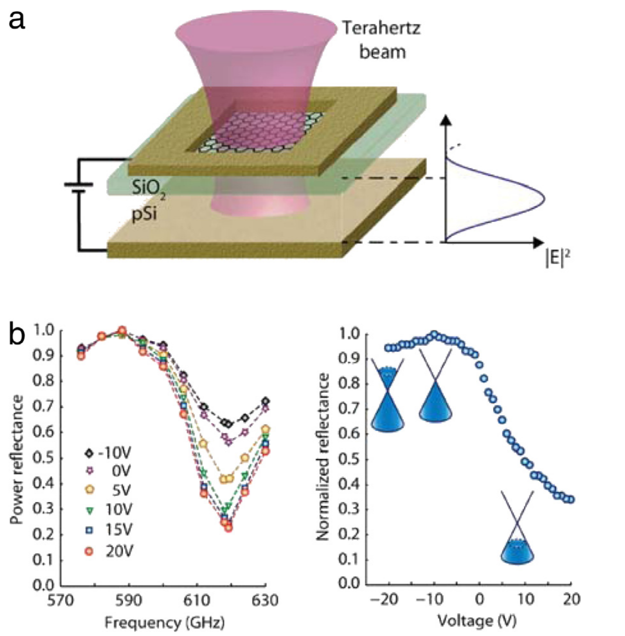

Fig. 2. (a) Sketch of a graphene-based reflectance modulator. The electric field intensity exhibits a node at the back contact, which also acts as a reflector. At the plane of graphene the electric field intensity depends on the substrate thickness and can be maximized when the substrate thickness is an odd multiple of a quarter wavelength. (b) Left panel: power reflectance as a function of frequency for different bias voltages; around 580–590 GHz the power reflectance is maximum and invariant since, at these frequencies, the substrate thickness is an even multiple of one-quarter of the terahertz wavelength; near 620 GHz the power reflectance is minimum and voltage tunability is observed. Right panel: normalized reflectance ($R/R(V_{CNP})$) at 620 GHz; the Dirac point voltage V_{CNP} was found to be −10 V.
Source: Reprinted with permission from Ref. [50].

One step further is to integrate graphene with metamaterials and to take advantage of the electric field enhancement due to the metamaterial so to boost the light matter interaction in graphene [54–66]. However, as discussed by Yan et al., one should keep in mind that in these structures there is always a trade-off between the modulation depth, insertion loss and the bandwidth of modulation [66]. Early experimental work on graphene metamaterial modulators by Lee et al. showed very large (86%) modulation depth, but at the expenses of a large insertion loss (>10 dB) [65]. Later work by Valmorra et al. [67], reports a smaller insertion loss (∼3 dB) with a much smaller modulation depth of ∼12%. Another low-bias terahertz modulator based on the integration of split-ring resonator and a graphene layer was proposed by Degl'Innocenti [68]. Modulation in a broad spectral range (2.2–3.1 THz) with a modulation depth of up to 18% was observed in this structure. In this regard it is worth mentioning a theoretical study by Tamagnone et al., which discusses the fundamental limits on graphene modulator performance [33]. By means of exploring the complete design space, the trade-offs between insertion loss and modulation depth are explored, leading to a minimum attainable loss for each given modulation depth level as depicted in Fig. 3; from this analysis it is observed that 100% modulation depth with less than 4 dB insertion loss is non realizable.

A metamaterial terahertz modulator based on periodic gold slit arrays and utilizing graphene as an active load of tunable conductivity was initially proposed in [69] and experimentally demonstrated in [70]. A sketch of this structure is depicted in Fig. 4(a). The field enhancement in the graphene layer is attained via coherent radiation of the enhanced in-plane local-field in the slits, thus preserving the broadband terahertz modulation of bare graphene in the hybrid device. Therefore this structure is capable of efficiently coupling terahertz radiation while exhibiting tunability

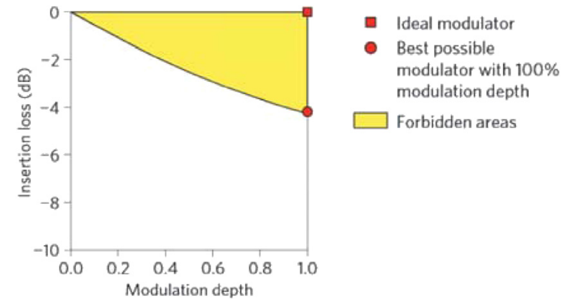

Fig. 3. Performances of terahertz modulators (modulation depth versus insertion loss). The square represents ideal modulators, and the circle denotes the best possible modulator with 100% modulation depth. Forbidden areas, non-realizable designs, are depicted in yellow.
Source: Reprinted with permission from Ref. [33].

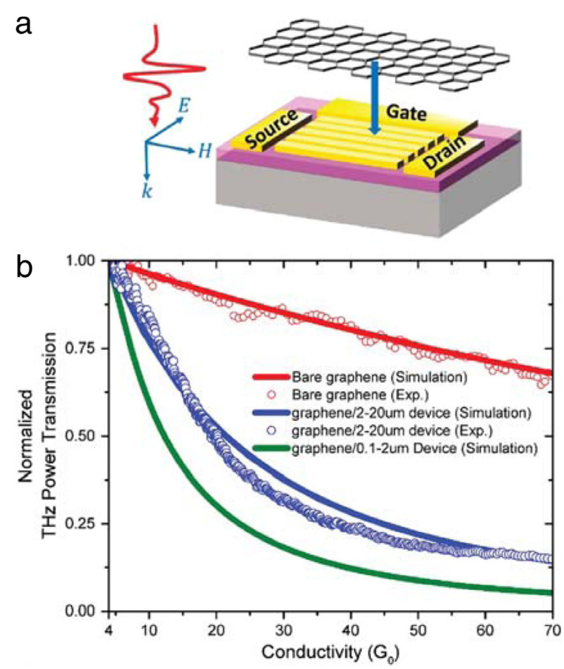

Fig. 4. (a) Schematic of a graphene/gold-slit-array hybrid device configuration. The incoming terahertz wave is polarized perpendicular to the slit orientation. (b) Normalized terahertz power transmission modulation as a function of graphene conductivity. The solid line traces are simulation results for bare graphene (red) and the hybrid device (blue). The empty dots are experimental data for bare graphene (red) and the hybrid device (blue, magenta). (For interpretation of the references to colour in this figure legend, the reader is referred to the web version of this article.)
Source: Reprinted with permission from Ref. [70].

of the terahertz transmission over a broad frequency range as shown in Fig. 4(b). Under this scheme strong terahertz absorption and a large local field enhancement exist, leading to a modulation depth of 90%. It is also possible to improve the modulation depth in these structures by increasing the number of graphene layers, the trade-off is that as the number of layers increases the insertion loss also increases. For example, in 2015, Wu et al. [71] reported on a broadband terahertz modulator based on graphene/ionic liquid/graphene sandwich structures, as shown in Fig. 5(a). The modulation depth obtained reached up to 99% in the frequency range 0.1–2.5 THz. Moreover, it is observed that the modulation depth improves as the number of stacked graphene pairs increases (see Fig. 5(b)).

Another recently proposed approach towards high-performance graphene modulators includes the use of hybrid systems in which by optically pumping the structure, the properties of the graphene

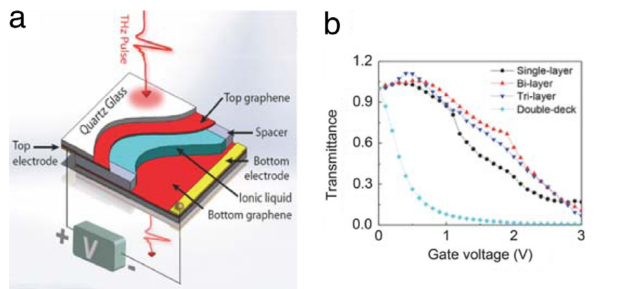

Fig. 5. (a) Geometry of an ionic-liquid-based graphene-based terahertz modulator: the sandwich structure consists of two quartz glasses coated with graphene films, two spacers, and an ionic liquid. The spacers are located at the edges of the quartz glasses so to support the graphene cavity with the ionic liquid. Cr/Au electrodes are deposited at one edge of each graphene film. (b) Comparison of terahertz modulation in devices with different number of graphene layers (single-layer, bilayer, and trilayer) showing a similar modulation depth in all cases. The double-deck device, which attains a larger modulation depth, is fabricated by stacking different bilayer and trilayer graphene devices.
Source: Reprinted with permission from Ref. [71].

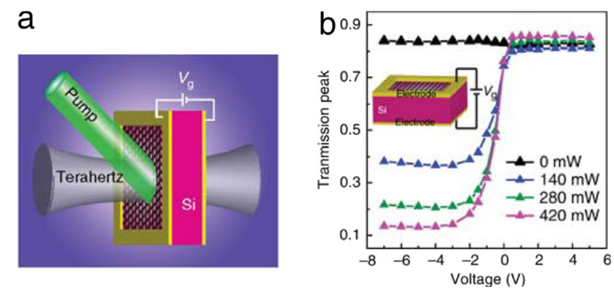

Fig. 6. (a) Schematic of a graphene–silicon terahertz diode. The double-layer graphene, which lies on top of the silicon substrate, was photoexcited with green light and biased with a voltage V_g. (b) Gate- and photoexcitation-controlled amplitude change of the normalized time-domain transmission peaks in the double-layer graphene on silicon device depicted in (a). (For interpretation of the references to colour in this figure legend, the reader is referred to the web version of this article.)
Source: Originally published in [79] under CC BY 4.0 license.

layer are altered and thus by properly engineering the device it is possible to obtain significant modulation depth [72,73]. A graphene terahertz modulator based on an optical pumping approach was demonstrated by Wen et al. in [73]. This terahertz modulator was based on single-layer graphene on germanium. The modulator was driven optically with a low power 1.55 μm laser. The authors claim that the main mechanism enabling terahertz modulation is the third order nonlinear effect [74–76] in the optical conductivity of the graphene. The modulator shows wide-band modulation in the range 0.25–1 THz with a modulation depth up to 94%.

A terahertz wave modulator employing waveguide-integrated geometries was proposed in [77]. The modulation depth in these structures is expected to be >38 dB based on simulations showing an excellent ON-state transmission (low insertion loss). Yet, another approach includes the integration of graphene in more complex systems. In [78], Liang et al. demonstrated that >94% modulation depth can be attained via the monolithic integration of a surface-emitting terahertz quantum cascade laser featuring a concentric circular grating with modulation speeds up to 110 MHz (∼3 orders magnitude faster than previous graphene-based terahertz modulators). The improvement in performance and speed is achieved as a result of the small area of the resulting device, and stronger interaction of the terahertz radiation with the graphene layer due to monolithic integration of modulator and source.

Finally it is worth mentioning that optical excitation and DC bias could be employed together as actuation mechanism. In a very recent study by Li et al. [79], a graphene–silicon hybrid device was experimentally demonstrated. This device, which poses a 'diode' behaviour is actuated under simultaneous CW photoexcitation and DC bias voltage as shown in Fig. 6((a)–(b)). This new graphene–silicon configuration exhibited a relatively large modulation depth of up to 83% at a low gate bias voltage of 4 V.

2.2. Phase modulation

Graphene can be also employed as a reconfigurable material enabling phase modulation at terahertz frequencies, which is also of interest for communications applications. Several devices have been proposed as terahertz phase modulators. Early device proposals consist of hybrid graphene/metal structures composed, namely, of: (a) a metallic metasurface, which provides a sharp resonance, and (b) a layer of graphene, which when a bias voltage is applied can provide tunability in to the device [44,80,81]. In these structures, it can be observed, as discussed by Chen et al. [82], that the terahertz transmission amplitude and phase through the graphene/metal hybrid structure are not independent of each other, but they are related by Kramers–Kronig(KK) relations. Near frequencies where maximum amplitude modulation is achieved no phase modulation takes place. In contrast, near frequencies where there is no amplitude modulation (i.e. the transmission amplitude is independent of the bias voltage), the phase experiences maximum shift. From this point of view at the frequencies where maximum modulation of phase is obtained there is no amplitude modulation, which makes these structures attractive as phase modulators. Moreover, a later theoretical study also showed that by using a planar graphene plasmonic waveguide, phase shifting is possible [83]. In terms of experimental demonstrations, Lee et al. reported on a multilayer structure composed of a metallic metasurface (honeycomb lattice) on top of a graphene layer; two extraordinary transmission electrodes are placed on both sides of this layered structure so to gate graphene. A sketch of the device structure is depicted in Fig. 7(a). Shown in Fig. 7(b) is the phase shift versus applied bias in this structure, a 65° phase shift is observed at a frequency of 0.9 THz [65]. Another potential structure enabling phase manipulation consist of periodically arranged graphene squares as theoretically proposed by Carrasco et al. [84]. Moreover, in this structure, via independently tuning the Fermi level in graphene in each of the square patches, reflect-arrays can be engineered, which might find use in beam shaping applications.

3. Graphene-based terahertz emitters

Currently available terahertz sources can be categorized in three groups: (i) *electronic-based sources*. These sources are typically used at millimetre-wave and microwave frequencies. Their operation is limited by reactive parasitics and/or the intrinsic electron transient time. Moreover, the attainable output power levels roll off at high frequencies, which makes them inefficient at frequencies above 1 THz [85]. (ii) *tube-sources*, which, although can operate at larger frequencies in the terahertz band than electronic-based sources, face the problem of being non-contact and a need for very high fields [86,87]. (iii) *solid-state (quantum cascade) lasers*, as used in the IR range. These sources are not efficient at room temperature, and cryogenic operation is required. This is owed to terahertz photons being associated with ∼meV energies, thus energy levels that are comparable to phonon energies in the lattice.

Nowadays, most terahertz sources operate by frequency conversion either from a lower frequency range (frequency multiplication), or from a higher frequency range (photomixing) [5]. From this perspective, new materials with extraordinary electro-optical properties, such as graphene, might provide a solution to these limitations.

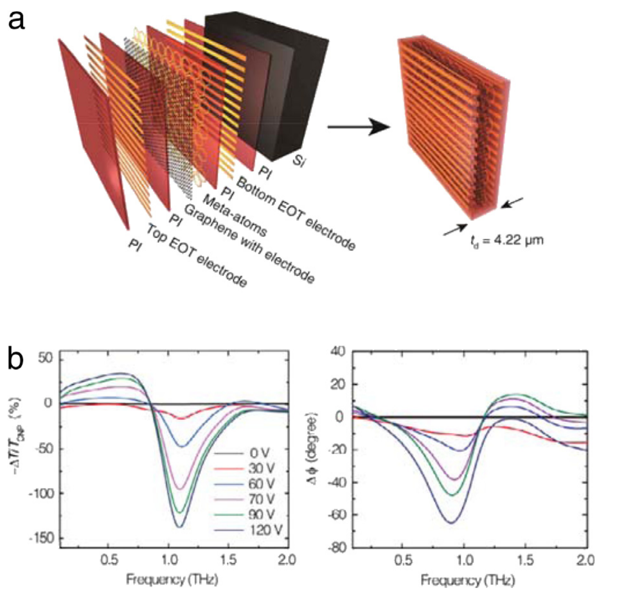

Fig. 7. (a) Detail of the stacked structure of a graphene-based metamaterial, which shows a strong phase modulation at 0.9 THz. (b) Right panel: fractional change on transmission as a function of frequency. Left panel: phase modulation as a function of frequency.
Source: Reprinted with permission from Ref. [65].

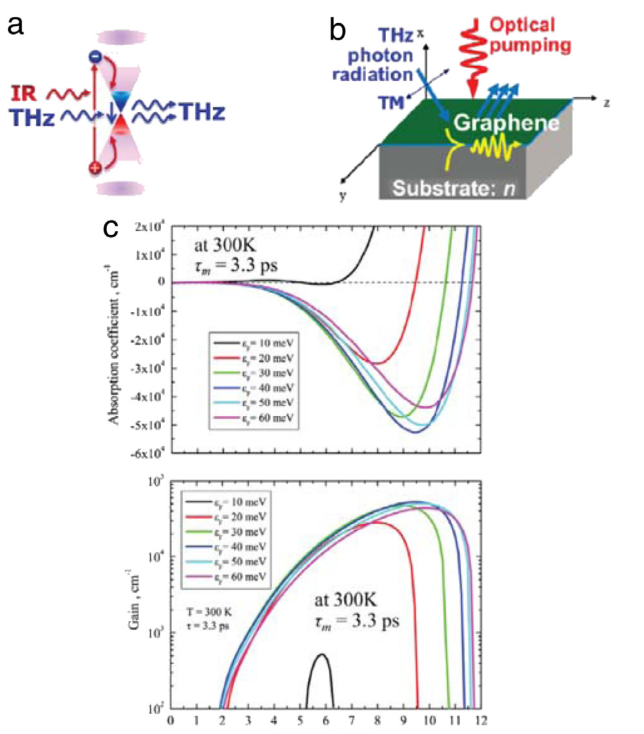

Fig. 8. (a) Schematic image of the stimulated terahertz emission in IR-pumped graphene. (b) Sketch of excitation of terahertz SPPs in a population inverted graphene layer. (c) Frequency dependences of SPP absorption (left) and gain (right) for monolayer population-inverted graphene on SiO_2/Si substrate at 300 K for different quasi-Fermi energies. Very large terahertz gain (negative values of absorption) of the order of 10^4 cm^{-1} is possible in such configuration.
Source: Originally published in [88] under CC BY 3.0 license.

Early work by Ryzhii et al. shows that interband population inversion can be achieved in graphene both by optical pumping (Fig. 8(a)) or carrier injection, e.g. [89,90]. Later, a graphene photonic laser based on dielectric and slot-line waveguides was pro-

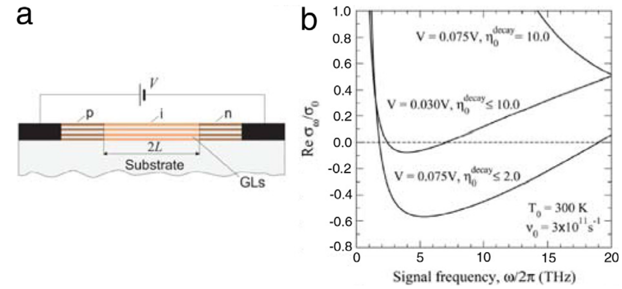

Fig. 9. (a) Schematic cross-sectional view of a proposed multi-graphene-layer terahertz laser with chemically doped n- and p-sections. (b) Example dynamic conductivity versus frequency showing the possibility of attaining negative dynamic conductivity in such structures.
Source: Reprinted with permission from Ref. [95].

posed [91]. Stimulated emission of terahertz and IR photons from population inversion in graphene was experimentally observed in these structures [92,93]. However, there is a fundamental limitation in these graphene terahertz lasers, which is related to the quantum conductance of graphene, i.e. the interband absorption by a monolayer of graphene is limited to $\frac{e^2}{4\hbar} = 2.3\%$ [94]. In order to overcome this limitation, there are several approaches that can be followed. One of them is to increase the number of graphene layers, which in turn will increase the absorption. However, in Ref. [91] it is shown that by following this approach the absorption coefficient still remains low, i.e. in the order of 1 cm^{-1} with 20 layers of graphene. Another approach is via using a waveguide, so that photons can propagate in the plane of graphene instead of at normal incidence into it, and thus maximize gain and overcome the quantum limitation in vertical cavity structures. A third approach consists in using Surface Plasmon Polaritons (SPPs) in graphene as depicted in Fig. 8(b); the fact that the plasmonic group velocity in graphene is several orders of magnitude smaller than the group velocity of a free-space wave can boost the light-matter interaction when a plasmonic wave is excited in graphene. This will cause the gain coefficient of plasmonic structures to be several order of magnitude larger than the gain in photonic structures. Excitation and propagation of SPPs along population inverted graphene sheets has been studied in Ref. [88], where it is shown that the localization of SPPs and their small group velocity leads to large gains as depicted in Fig. 8(c). Moreover, based on the population inversion in graphene layers, a current-injection terahertz laser was also proposed [95]. A sketch of the structure is depicted in Fig. 9(a). The structure is based on a p–i–n junction. Population inversion can be achieved by applying a voltage between source and drain (see Fig. 9(b)). The electrons and holes can recombine by means of an optically-assisted interband transition which result in spontaneous terahertz photon emission when the applied voltage is in the order of couple of mV to tens of mV. Moreover, plasmon emission was also demonstrated in a suspended graphene sheet due to carrier recombination [96]. Picosecond photocurrent is observed in a suspended sample with a stripline metal contact, i.e. by applying electric field to the metal graphene contact a photocurrent along with a photothermoelectric current is generated. It is shown that if the sample is optically pumped, electromagnetic radiation can be generated up to 1 THz.

4. Graphene-based terahertz detectors

Besides communications applications, photodetection of terahertz radiation is relevant for a variety of strategic spectroscopic applications, ranging from biological applications, medical diagnostics, pharmaceutical sciences, to process control and homeland security [4,97]. Conventional terahertz and sub-THz detection systems based on incoherent (pyroelectric, Golay cell, Si bolometers) or coherent (heterodyne mixers) approaches are either very slow (∼100 Hz modulation frequency) or require deep cryogenic cooling, while those exploiting fast nonlinear electronics (Schottky diodes) show a significant drop of performance above 1 THz [98]. Recently, room temperature field effect transistors have been shown capable of detecting terahertz waves in the 0.3–3 THz range based on InAs nanowire FETs [99,100]. These detectors have shown very fast response and high responsivities [101], and have also been implemented in multi-pixel focal plane arrays for imaging applications [102].

In a series of pioneering papers [103–106], Dyakonov and Shur proposed a mechanism enabling detection of terahertz radiation, which is based on the fact that a FET hosting a two-dimensional electron gas (2DEG) can act as a resonant cavity for electron plasma waves. According to the Dyakonov–Shur scheme, a plasma wave is launched by modulating the carrier density and velocity by an incoming terahertz wave coupled by an antenna structure. Due to the nonlinearities in the electron transport, the terahertz electric field is rectified like in square law detectors thus a constant (DC) source to drain photovoltage is induced. When the electron plasma wave is launched at the source terminal of the FET, it might reach the drain terminal in a time shorter than the electron momentum relaxation time (τ), or, $\omega\tau > 1$ and $L < s\tau$, where L is the channel length, s is the plasma wave velocity, in this case the device photoresponse will be resonant [101,105,106]. This condition requires electron mobility to be in the order of several thousands cm^2/Vs at frequencies >1 THz. Broadband detection occurs, when the electron plasma wave is overdamped or when the channel length of the FET is larger than the length over which plasma waves can travel [101,105–107]. This regime has the advantage that the responsivity can be maximized with the gate bias V_g (while measuring the output at the drain with no source–drain bias applied), thus dramatically improving the signal to noise ratio (SNR). Resonant photodetection is still to be fully demonstrated at room temperature, although some suggestive evidences have been reported in HEMTs [108,109]. However, still, the large, spectrally sharp, and tunable responsivity enhancements, with respect to the non-resonant case, are yet to be achieved. High mobility at room temperature is therefore crucial to take full advantage of resonant detection.

Recently, it has been understood that graphene can pave the way for the realization of robust and cheap terahertz detectors operating at room temperature and based on the Dyakonov and Shur scheme [97,110]. Graphene has indeed such a high carrier mobility, even at room temperature [111]. Furthermore, it supports plasma waves that are weakly damped in high-quality samples [112,113]. Thus, single-layer (SL) and bilayer (BL) graphene FET (GFET) plasma-based photodetectors could outperform other terahertz detector technologies. In the last couple of years, various graphene based structures have been proposed i.e. SL or BL graphene–insulator–graphene heterostructure tunnel FET (GIG TFET) [114–120], vertical graphene-based hot-electron transistors [121], lateral SL or BL GFET [122], vertical cascade multiple graphene layer structures [123], etc., for resonant detection. The plasma properties of a 2DEG become more pronounced with decreasing effective masses and increasing electron mobility [97]. Although the dispersion of plasma waves in gated graphene is strongly nonlinear and density dependent, for fairly long wavelengths compared to the gate-graphene distance, a linear approximation holds quite well. The resulting plasma velocity (s) considerably exceeds that of electrons (holes) in III–V 2DEGs. As a result the quality factor Q determining the sharpness of the plasma resonances $Q = \omega\tau$ is directly linked to the mobility μ, meaning that graphene-based heterostructures with elevated mobilities should show very pronounced plasma resonances.

A promising graphene device consists of a GIG TFET as reported in [114]. Such devices have been fabricated and characterized —

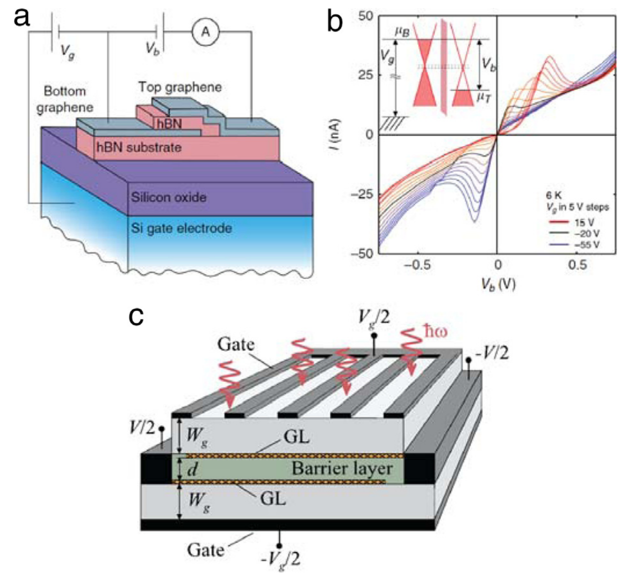

Fig. 10. (a) Schematic of a Graphene–Insulator–Graphene resonant tunnelling transistor, and (b) measured current–voltage characteristics of such a device; the inset shows schematically the relative positions of the Fermi energies of the two graphene layers at the peak of the $I(V)$ curve. Originally published in [117] under CC BY 3.0 license. (c) Schematic view of a GIG TFET structure with "electrical doping" and top gate serving as the grating coupler.
Source: Reprinted with permission from Ref. [120].
© 2014, American Institute of Physics.

using both SL and BL graphene [see Fig. 10(a) and (b)]. The DC and RF characteristics for such devices have been extensively studied [114–120,124–126] and both SL and BL GIG TFETs show negative differential conductance as depicted in Fig. 10(b) [117–119]. Recent works demonstrate that such GIG TFET structures can show strong resonant terahertz detection, compared to ungated GIG TFET structures, see Refs. [115,116,124]. The developed analytical model clearly shows that at frequencies close to ω_p (resonant frequency) or its harmonics, the detector responsivity exhibits sharp maxima provided the plasma oscillation quality factor $Q >> 1$. Since, the electron plasma wave group velocity (s) depends on bias voltage V_g and ω_p depends on s and L (graphene length), hence the responsivity peak can be tuned by means of either changing V_G or L. Efficient coupling of the terahertz radiation into plasmons in these structures can be done using grating gate topologies as depicted in Fig. 10(c) [120].

Graphene has also been proposed for broadband terahertz detection by employing a simple top-gate antenna-coupled configuration for the excitation of overdamped plasma waves in the channel of a GFET [110]. Log-periodic circular toothed as well as bow-tie antennas has been used for 0.29–0.4 THz, 2 and 4 THz radiation detection [110,128,129]. Similarly split-bow tie antenna has also been used to improve the coupling and hence responsivity at 0.6 THz [127]. The photovoltage in this type of devices is proportional to the derivative of the channel conductivity with respect to V_G, according to the phenomenological formula from the diffusive theoretical model [130,131]:

$$\Delta U \propto \left[\frac{1}{\sigma}\frac{d\sigma}{dU}\right]_{U=V_g}.$$

Fig. 11(a) and (b) plots Rv (voltage responsivity) measured in exfoliated SL and BL graphene on Si/SiO_2 FETs at room temperature, for 0.3 THz, while sweeping V_g from −1 to +3.5 V and modulating the terahertz source at 500 Hz [110]. Each SL curve in Fig. 11(a) corresponds to a different relative orientation between the source electric-field polarization and the antenna axis. In the case of the SL device the photoresponse drops rapidly

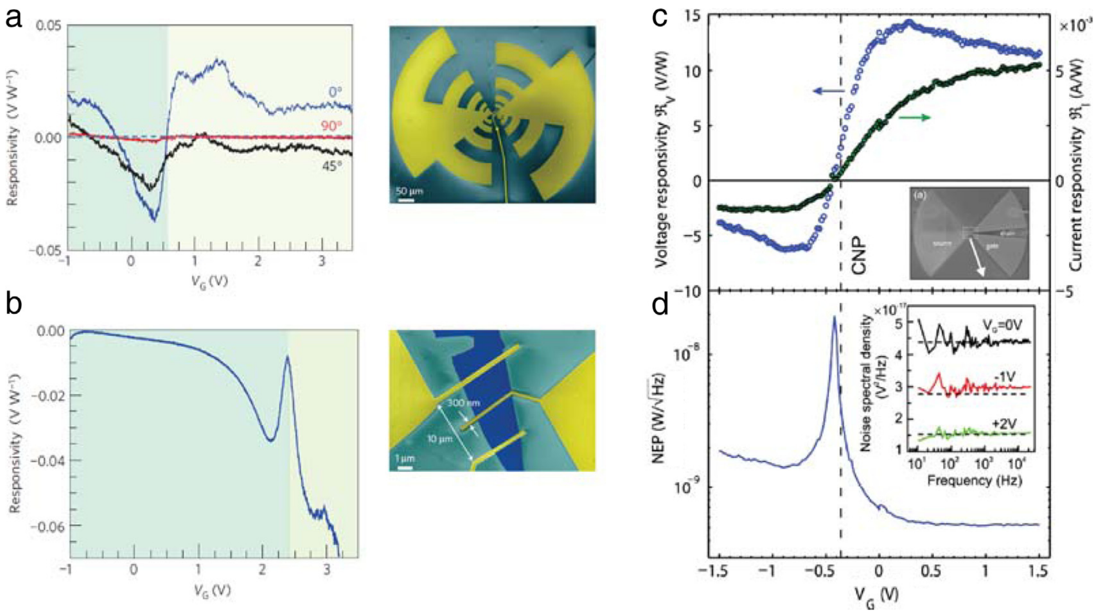

Fig. 11. Room temperature responsivity as a function of gate bias (V_g) for terahertz detectors based on (a) SL-GFET (with data for different angles between the beam polarization axis and the antenna axis), and, (b) BL-GFET (detail). The detectors depicted in (a) and (b) consist of a log-periodic circular-toothed antenna between source and gate, different background colours identify regions below and above the Dirac point. Reprinted with permission from Ref. [110]. Copyright 2012 Nature Publishing Group. (c) SL-GFET with a split bow-tie antenna patterned, and, (d) NEP for SL-GFET with a split bow-tie antenna patterned. (For interpretation of the references to colour in this figure legend, the reader is referred to the web version of this article.)
Source: Reprinted with permission from Ref. [127].
© 2014, American Chemical Society. Insets: SEM micrographs of the fabricated devices with respective antenna structures.

with angle until it becomes almost zero when the incoming polarization is orthogonal to the antenna axis, confirming the efficacy of the dipole antenna. Fig. 11(c) and (d) plots Rv and NEP (noise equivalent power) measured in CVD grown SL on Si/SiO_2 FETs at room temperature, for 0.6 THz, while sweeping V_G from -1.5 to $+1.5$ V [127]. Together with the expected photovoltage change in the vicinity of the Dirac point, a further sign switch is observed in all cases, suggesting a possible contribution of photo-thermoelectric origin [132,133]. Similar results were obtained for detection at 1.63 and 3.11 THz using graphene FETs, where the drain and source contact leads worked as antennas for the incoming terahertz radiation [133].

As per other experimental work on graphene based terahertz detectors is concerned, several processes of photocurrent generation contribute in biased graphene, namely: (a) the photo thermoelectric Seebeck effect, (b) the photovoltaic effect, and (c) the photo-induced bolometric effect. Device operation based on all these three processes has been demonstrated in the mid-infrared and far infrared regimes [134]. In the bolometric process, the incident electromagnetic radiation raises the local temperature of graphene, which alters the resistance of the device, producing a change in DC current under bias. Recent work based on dual gated bilayer graphene (DGBLG) hot-electron bolometer (HEB) operation is reported in Ref. [135]. Fig. 12(a) shows the schematic and Fig. 12(b) shows the photoresponse, of this device. In Ref. [135] BL graphene was used as BL graphene small electron heat capacity and weak electron–phonon coupling/interaction creates a bottleneck in the heat path, thus gives rise to a temperature dependent resistance (ΔR) induced by the large change in electron temperature. This photon absorption-induced ΔR is then converted to a detectable electrical signal. The photoresponse in this device at terahertz frequency, has a photovoltaic contribution as well [136], but the photoresponse is dominated by the bolometric effect for gapped BL graphene, with majority of the optical energy being lost to hot electrons and then to acoustic phonons. Electrons do not pass the energy to optical phonons even though the optical energy is higher than the optical phonon energy as theoretical and experimental results indicate that the electron–electron scattering rate is higher than the electron–phonon scattering rate and electrons tend to thermalize among themselves before passing the energy to other degrees of freedom. The developed detector exhibits a voltage responsivity of about $2 \times 10^5 VW^{-1}$ and an electrical NEP of about 33 $fWHz^{-1/2}$ at 5 K. A high intrinsic speed of the device (>1 GHz at 10 K) is also demonstrated (see Fig. 12(c)).

Room temperature terahertz detection using the photothermoelectric effect (PTE) in graphene has also been shown experimentally recently [137–139]. In photothermoelectric processes, a laser spot produces a temperature gradient in the device, which together with a doping asymmetry generates a thermoelectric current [134]. The hot-electron PTE in graphene is a promising detection mechanism; photoexcited carriers rapidly thermalize due to strong electron–electron interactions, but lose energy to the lattice more slowly. The electron temperature gradient drives electron diffusion, and asymmetry due to local gating or dissimilar contact metals produces a net current via the thermoelectric effect. Sign reversal of photoresponse with gate voltage also indicates the existence of PTE [132,133]. Fig. 13(a) shows, the optical micrograph of an optimally coupled graphene photothermoelectric detector device fabricated using exfoliated SL graphene. The graphene thermoelectric terahertz photodetector exhibits voltage responsivity of about 700 VW^{-1} at room temperature (see Fig. 13(b)) and NEP of about 20 $pWHz^{-1/2}$, referenced to the incident (absorbed) power. Fig. 13(c) shows another device with multiple graphene channels so to enhance the signal. A significant advantage of this device is its speed; Fig. 13(d) shows, for the device depicted in Fig. 13(c), the electrical impulse response to terahertz excitation, which is found to be ∼110 ps. Similar results were obtained at higher frequencies up to 8 THz utilizing a tunable plasmonic resonance in subwavelength graphene nanoribbons to increase absorption efficiency [138]. In this work [138], by using dissimilar metal electrodes, a photothermoelectric detector was formed with tilted

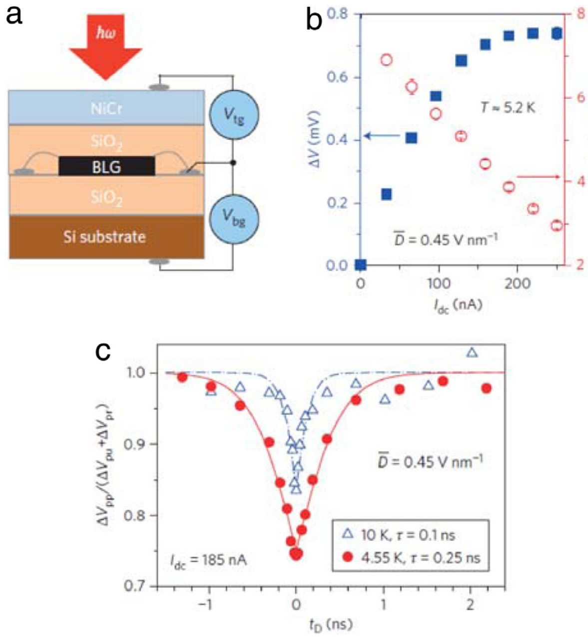

Fig. 12. (a) Schematic of a bolometer device geometry with electric-field-effect gating (DGBLG HEB). (b) Photoresponse of a DGBLG HEB, Blue squares represent the photoresponse and red circles represent the electrical resistance $\Delta R = \Delta V/I_{DC}$. (c) Response time of the DGBLG HEB.
Source: Reprinted with permission from Ref. [135].
© 2012, Nature Publishing Group.

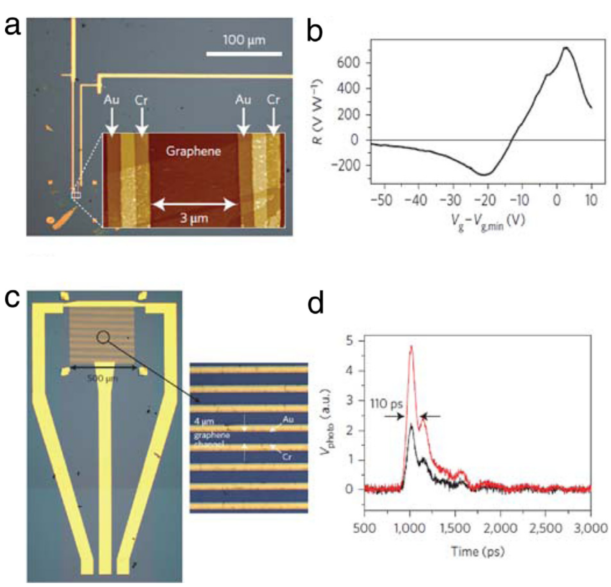

Fig. 13. (a) Optical micrograph showing the electrical contact of a graphene photothermoelectric detector. (b) Responsivity to 119 μm wavelength terahertz radiation for the device depicted in Fig. 4(a). (c) Micrograph of a device with multiple graphene channels. (d) Time-domain photoresponse to pulsed laser excitation for the device depicted in Fig. 4(c).
Source: Reprinted with permission from Ref. [137].
© 2014, Nature Publishing Group.

graphene microribbon array. An enhanced photovoltage at room temperature was observed when the carrier density of graphene is tuned such that, the plasmon resonance frequency matches the continuous-wave terahertz excitation.

5. Conclusion

Graphene has a great potential to revolutionize terahertz communications applications in decades to come. In a span of just a few years graphene has shown state-of-the-art modulator performances, and graphene-based detectors are also rapidly approaching the performance of state-of-the-art terahertz technologies. As for generation of terahertz waves, the potential of graphene is instead almost completely unexplored. Although many theoretical proposals of graphene based terahertz sources have recently arisen, conclusive experimental demonstrations are still lacking. In addition, it is expected that a myriad of technological possibilities will open up when graphene devices are integrated with existing technologies.

Acknowledgements

This work was supported by NSF awards: ECCS #1407959, DMR #1121252, and the NSF CAREER award #1351389.

References

[1] S. Cherry, Edholm's law of bandwidth, IEEE Spectr. 41 (7) (2004) 58–60.
[2] S. Ho-Jin, T. Nagatsuma, Present and future of terahertz communications, IEEE Trans. Terahertz Sci. Technol. 1 (1) (2011) 256–263.
[3] D. Saeedkia (Ed.), Handbook of Terahertz Technology for Imaging, Sensing and Communications, Elsevier, 2013.
[4] I.F. Akyildiz, J.M. Jornet, C. Han, Terahertz band: Next frontier for wireless communications, Phys. Commun. 12 (2014) 16–32.
[5] M. Tonouchi, Cutting-edge terahertz technology, Nat. Photonics 1 (2007) 97–105.
[6] R. Piesiewicz, T. Kleine-Ostmann, N. Krumbholz, D. Mittleman, M. Koch, J. Schoebel, T. Kurner, Short-range ultra-broadband terahertz communications: Concepts and perspectives, IEEE Antennas Propag. Mag. 49 (6) (2007) 24–39.
[7] J. Federici, L. Moeller, Review of terahertz and subterahertz wireless communications, J. Appl. Phys. 107 (2010) 111101.
[8] D. Grischkowsky, S. Keiding, M. van Exter, Ch. Fattinger, Far-infrared time-domain spectroscopy with terahertz beams of dielectrics and semiconductors, J. Opt. Soc. Amer. B 7 (1990) 2006–2015.
[9] K.S. Novoselov, D. Jiang, F. Schedin, T.J. Booth, V.V. Khotkevich, S.V. Morozov, A.K. Geim, Two-dimensional atomic crystals, Proc. Natl. Acad. Sci. 102 (2005) 10451–10453.
[10] A.K. Geim, Graphene prehistory, Phys. Scr. T 146 (2012).
[11] A.E. Karu, M. Beer, Pyrolytic formation of highly crystalline graphite films, J. Appl. Phys. 37 (1966) 2179–2181.
[12] A.N. Obraztsov, E.A. Obraztsova, A.V. Tyurnina, A.A. Zolotukhin, Chemical vapor deposition of thin graphite films of nanometer thickness, Carbon 45 (10) (2007) 2017–2021.
[13] S. Bae, H. Kim, Y. Lee, X. Xu, J.-S. Park, Y. Zheng, J. Balakrishnan, T. Lei, H.R. Kim, Y.I. Song, Y.-J. Kim, K.S. Kim, B. Özyilmaz, J.-H. Ahn, B.H. Hong, S. Iijima, Roll-to-roll production of 30-inch graphene films for transparent electrodes, Nature Nanotechnol. 4 (2010) 574–578.
[14] R. Muñoz, C. Gómez-Aleixandre, Review of CVD synthesis of graphene, Chem. Vapor Depos. 19 (2013) 297–322.
[15] J.W. Suk, A. Kitt, C.W. Magnuson, Y. Hao, S. Ahmed, J. An, A.K. Swan, B.B. Goldberg, R.S. Ruoff, Transfer of CVD-grown monolayer graphene onto arbitrary substrates, ACS Nano 5 (9) (2011) 6916–6924.
[16] J.D. Caldwell, T.J. Anderson, J.C. Culbertson, G.G. Jernigan, K.D. Hobart, F.J. Kub, M.J. Tadjer, J.L. Tedesco, J.K. Hite, M.A. Mastro, R.L. Myers-Ward, C.R. Eddy Jr., P.M. Campbell, D.K. Gaskill, Technique for the dry transfer of epitaxial graphene onto arbitrary substrates, ACS Nano 4 (2) (2010) 1108–1114.
[17] X. Liang, B.A. Sperling, I. Calizo, G. Cheng, C.A. Hacker, Q. Zhang, Y. Obeng, K. Yan, H. Peng, Q. Li, X. Zhu, H. Yuan, A.R. Hight Walker, Z. Liu, L.-M. Peng, C.A. Richter, Toward clean and crackless transfer of graphene, ACS Nano 5 (11) (2011) 9144–9153.
[18] Y. Lee, S. Bae, H. Jang, S. Jang, S.-E. Zhu, S.H. Sim, Y.I. Song, B.H. Hong, J.-H. Ahn, Wafer-Scale synthesis and transfer of graphene films, Nano Lett. 10 (2) (2010) 490–493.
[19] L. Gao, W. Ren, H. Xu, L. Jin, Z. Wang, T. Ma, L.-P. Ma, Z. Zhang, Q. Fu, L.M. Peng, X. Bao, H.-M. Cheng, Repeated growth and bubbling transfer of graphene with millimeter-size single-crystal grains using platinum, Nature Commun. 3 (2012) 699.
[20] A.K. Geim Novoselov, The rise of graphene, Nature Mater. 6 (2007) 183–191.
[21] X. Du, I. Skachko, A. Barker, E.Y. Andrei, Approaching ballistic transport in suspended graphene, Nature Nanotechnol. 3 (2008) 491–495.
[22] K.S. Novoselov, A.K. Geim, S.V. Morozov, D. Jiang, Y. Zhang, S.V. Dubonos, I.V. Grigorieva, A.A. Firsov, Electric field effect in atomically thin carbon films, Science 306 (2004) 666–669.
[23] Y.M. Lin, A.V. Garcia, S.J. Han, D.B. Farmer, I. Meric, Y. Sun, Y. Wu, C. Dimitrakopoulos, A. Grill, P. Avouris, K.A. Jenkins, Wafer-scale graphene integrated circuit, Science 332 (6035) (2011) 1294–1297.
[24] M.C. Lemme, T.J. Echtermeyer, M. Baus, H.A. Kurz, Graphene field effect device, IEEE Electron Device Lett. 28 (2007) 282–284.

[25] Y.-M. Lin, C. Dimitrakopoulos, K.A. Jenkins, D.B. Farmer, H.-Y. Chiu, A. Grill, Ph. Avouris, 100-GHz transistors from wafer-scale epitaxial graphene, Science 327 (2010) 662.
[26] F. Bonaccorso, Z. Sun1, T. Hasan, A.C. Ferrari, Graphene photonics and optoelectronics, Nat. Photonics 4 (2010) 611–622.
[27] B. Sensale-Rodriguez, R. Yan, L. Liu, D. Jena, H.G. Xing, Graphene for reconfigurable terahertz optoelectronics, Proc. IEEE 101 (7) (2013) 1705–1716.
[28] B. Sensale-Rodriguez, Graphene-based optoelectronics, J. Lightwave Technol. 33 (5) (2015) 1100–1108.
[29] T. Ando, Y. Zheng, H. Suzuura, Dynamical conductivity and zero-mode anomaly in honeycomb lattices, J. Phys. Soc. Japan 71 (2002) 1318–1324.
[30] B. Sensale-Rodriguez, T. Fang, R. Yan, M.M. Kelly, D. Jena, L. Liu, H.G. Xing, Unique prospects for graphene-based terahertz modulators, Appl. Phys. Lett. 99 (2011) 113104.
[31] X. He, S. Kim, Tunable terahertz graphene metamaterials, Carbon 86 (2015) 229–237.
[32] A. Tredicucci, M.S. Vitiello, Device concepts for graphene-based terahertz photonics, IEEE J. Sel. Top. Quantum Electron. 20 (1) (2014) 130–138.
[33] M. Tamagnone, A. Fallahi, J.R. Mosig, J. Perruisseau-Carrier, Fundamental limits and near-optimal design of graphene modulators and non-reciprocal devices, Nat. Photonics 8 (2014) 556–563.
[34] T. Otsuji, V. Popov, V. Ryzhii, Active graphene plasmonics for terahertz device applications, J. Phys. D: Appl. Phys. 47 (2014) 094006.
[35] P.-Y. Chen, H. Huang, D. Akinwande, A. Alù, Graphene-based plasmonic platform for reconfigurable terahertz nanodevices, ACS Photonics 1 (8) (2014) 647–654.
[36] F.J. García de Abajo, Graphene plasmonics: challenges and opportunities, ACS Photonics 1 (3) (2014) 135–152.
[37] M. Rahm, J.-S. Li, W.J. Padilla, THz wave modulators: a brief review on different modulation techniques, J. Infrared, Millim., Terahertz Waves 34 (1) (2013) 1–27.
[38] P.-Y. Chen, A. Alu, Terahertz metamaterial devices based on graphene nanostructures, IEEE Trans. Terahertz Sci. Technol. 3 (6) (2013) 748–756.
[39] H. Tanoto, L. Ding, J.H. Teng, Tunable terahertz metamaterials, Terahertz Sci. Technol. 6 (1) (2013) 1–25.
[40] S.H. Lee, H.-D. Kim, H.J. Choi, B. Kang, Y.R. Cho, B. Min, Broadband modulation of terahertz waves with non-resonant graphene meta-devices, IEEE Trans. Terahertz Sci. Technol. 3 (6) (2013) 764–771.
[41] Y. Zhou, X. Xu, H. Fan, Z. Ren, J. Bai, L. Wang, Tunable magnetoplasmons for efficient terahertz modulator and isolator by gated monolayer graphene, Phys. Chem. Chem. Phys. 15 (2013) 5084–5090.
[42] A. Andryieuski, A.V. Lavrinenko, Graphene metamaterials based tunable terahertz absorber: effective surface conductivity approach, Opt. Express 21 (7) (2013) 9144–9155.
[43] M. Amin, M. Farhat, H. Bagcı, A dynamically reconfigurable fano metamaterial through graphene tuning for switching and sensing applications, Sci. Rep. 3 (2013) 2105.
[44] B. Vasić, M.M. Jakovljević, G. Isić, R. Gajić, Tunable metamaterials based on split ring resonators and doped graphene, Appl. Phys. Lett. 103 (2013) 011102.
[45] K. Yang, S. Liu, S. Arezoomandan, A. Nahata, B. Sensale-Rodriguez, Graphene-based tunable metamaterial terahertz filters, Appl. Phys. Lett. 105 (9) (2014) 093105.
[46] Y. Bludov, V.N. MR Peres, M.I. Vasilevskiy, Unusual reflection of electromagnetic radiation from a stack of graphene layers at oblique incidence, J. Opt. 15 (11) (2013) 11404.
[47] J.-T. Liu, N.-H. Liu, L. Wang, X.-H. Deng, F.-H. Su, Gate-tunable nearly total absorption in graphene with resonant metal back reflector, Europhys. Lett. 104 (5) (2013) 57002.
[48] B. Sensale-Rodriguez, R. Yan, M.M. Kelly, T. Fang, K. Tahy, W.S. Hwang, D. Jena, L. Liu, H.G. Xing, Broadband graphene terahertz modulators enabled by intraband transitions, Nature Commun. 3 (2012) 780.
[49] I. Maeng, S. Lim, S.J. Chae, Y.H. Lee, H. Choi, J.-H. Son, Gate-controlled Nonlinear conductivity of dirac fermion in graphene field-effect transistors measured by terahertz time-domain spectroscopy, Nano Lett. 12 (2) (2012) 551–555.
[50] B. Sensale-Rodriguez, R. Yan, S. Rafique, M. Zhu, W. Li, X. Liang, D. Gundlach, V. Protasenko, M.M. Kelly, D. Jena, L. Liu, H.G. Xing, Extraordinary control of terahertz beam reflectance in graphene electro-absorption modulators, Nano Lett. 12 (9) (2012) 4518–4522.
[51] B. Sensale-Rodriguez, S. Rafique, R. Yan, M. Zhu, V. Protasenko, D. Jena, L. Liu, H.G. Xing, Terahertz imaging employing graphene modulator arrays, Opt. Express 21 (2) (2013) 2324–2330.
[52] L. Ju, B. Geng, J. Horng, C. Girit, M. Martin, Z. Hao, H.A. Bechtel, X. Liang, A. Zettl, Y.R. Shen, F. Wang, Graphene plasmonics for tunable terahertz metamaterials, Nature Nanotechnol. 6 (2011) 630–634.
[53] B. Sensale-Rodriguez, R. Yan, M. Zhu, D. Jena, L. Liu, H.G. Xing, Efficient terahertz electro-absorption modulation employing graphene plasmonic structures, Appl. Phys. Lett. 101 (26) (2012) 261115.
[54] X.-J. He, T.-Y. Li, L. Wang, J.-M. Wang, J.-X. Jiang, G.-H. Yang, F.-Y. Meng, Q. Wu, Electrically tunable terahertz wave modulator based on complementary metamaterial and graphene, J. Appl. Phys. 115 (2014) 17B903.
[55] Y. Zhang, Y. Feng, B. Zhu, J. Zhao, T. Jiang, Graphene based tunable metamaterial absorber and polarization modulation in terahertz frequency, Opt. Express. 22 (19) (2014) 22743–22752.
[56] J. Ding, B. Arigong, H. Ren, M. Zhou, J. Shao, M. Lu, Y. Chai, Y. Lin, H. Zhang, Tuneable complementary metamaterial structures based on graphene for single and multiple transparency windows, Sci. Rep. 4 (2014) 6128.
[57] Z. Wang, M. Zhou, X. Lin, H. Liu, H. Wang, F. Yu, S. Lin, E. Li, H. Chen, A circuit method to integrate metamaterial and graphene in absorber design, Opt. Commun. 329 (2014) 76–80.
[58] B. Grześkiewicz, A. Sierakowski, J. Marczewski, N. Pałka, E. Wolarz, Polarization-insensitive metamaterial absorber of selective response in terahertz frequency range, J. Opt. 16 (10) (2014) 105104.
[59] L. Wang, X. Chen, A. Yu, Y. Zhang, J. Ding, W. Lu, Highly sensitive and wide-band tunable terahertz response of plasma waves based on graphene field effect transistors, Sci. Rep. 4 (2014) 5470.
[60] N. Born, M. Scheller, M. Koch, J.V. Moloney, Cavity enhanced terahertz modulation, Appl. Phys. Lett. 104 (2014) 103508.
[61] B. Wang, X. Zhang, K.P. Loh, J. Teng, Tunable broadband transmission and phase modulation of light through graphene multilayers, J. Appl. Phys. 115 (2014) 213102.
[62] R. Kowerdziej, M. Olifierczuk, J. Parka, J. Wróbel, Terahertz characterization of tunable metamaterial based on electrically controlled nematic liquid crystal, Appl. Phys. Lett. 105 (2014) 022908.
[63] Q. Mao, Q.-Y. Wen, W. Tian, T.-L. Wen, Z. Chen, Q.-H. Yang, H.-W. Zhang, High-speed and broadband terahertz wave modulators based on large-area graphene field-effect transistors, Opt. Lett. 39 (19) (2014) 5649–5652.
[64] X. He, H. Lu, Graphene-supported tunable extraordinary transmission, Nanotechnology 25 (32) (2014) 325201.
[65] S.H. Lee, M. Choi, T.-T. Kim, S. Lee, M. Liu, X. Yin, H.K. Choi, S.S. Lee, C.-G. Choi, S.-Y. Choi, X. Zhang, B. Min, Switching terahertz waves with gate-controlled active graphene metamaterials, Nature Mater. 11 (2012) 936–941.
[66] R. Yan, B. Sensale-Rodriguez, L. Liu, D. Jena, H.G. Xing, A new class of tunable metamaterial terahertz modulators, Opt. Express 20 (27) (2012) 28664–28671.
[67] F. Valmorra, G. Scalari, C. Maissen, W. Fu, C. Schönenberger, J.W. Choi, H.G. Park, M. Beck, J. Faist, Low-Bias active control of terahertz waves by coupling large-area CVD graphene to a Terahertz metamaterial, Nano Lett. 13 (7) (2013) 3193–3198.
[68] R. Degl'Innocenti, D.S. Jessop, Y.D. Shah, J. Sibik, J.A. Zeitler, P.R. Kidambi, S. Hofmann, H.E. Beere, D.A. Ritchie, Low-bias terahertz amplitude modulator based on split-ring resonators and graphene, ACS Nano 8 (3) (2014) 2548–2554.
[69] A. Novitsky, A.M. Ivinskaya, M. Zalkovskij, R. Malureanu, P. Uhd Jepsen, A.V. Lavrinenko, Non-resonant terahertz field enhancement in periodically arranged nanoslits, J. Appl. Phys. 112 (2012) 074318.
[70] S.-F. Shi, B. Zeng, H.-L. Han, X. Hong, H.-Z. Tsai, H.S. Jung, A. Zettl, M.F. Crommie, F. Wang, Optimizing broadband terahertz modulation with hybrid graphene/metasurface structures, Nano Lett. 15 (1) (2015) 372–377.
[71] Y. Wu, C. La-o-vorakiat, X. Qiu, J. Liu, P. Deorani, K. Banerjee, J. Son, Y. Chen, E.E.M. Chia, H. Yang, Graphene terahertz modulators by ionic liquid gating, Adv. Mater. 27 (11) (2015) 1874–1879.
[72] P. Weis, J.L. Garcia-Pomar, M. Höh, B. Reinhard, A. Brodyanski, M. Rahm, Spectrally wide-band terahertz wave modulator based on optically tuned graphene, ACS Nano 6 (10) (2012) 9118–9124.
[73] Q.-Y. Wen, W. Tian, Q. Mao, Z. Chen, W.-W. Liu, Q.-H. Yang, M. Sanderson, H.-W. Zhang, Graphene based all-optical spatial terahertz modulator, Sci. Rep. 4 (2014) 7409.
[74] S.A. Mikhailov, Non-linear electormagnetic response if graphene, Europhys. Lett. 79 (2007) 27002.
[75] S.A. Mikhailov, Non-linear graphene optics for terahertz applications, Microelectron. J. 40 (2009) 712–715.
[76] K. Yang, S. Arezoomandan, B. Sensale-Rodriguez, The linear and nonlinear thz properties of graphene, Terahertz Sci. Technol. 6 (4) (2013) 223–233.
[77] I. Khromova, A. Andryieuski, A. Lavrinenko, Ultrasensitive terahertz/infrared waveguide modulators based on multilayer graphene metamaterials, Laser Photonics Rev. 8 (6) (2014) 916–923.
[78] G. Liang, X. Hu, X. Yu, Y. Shen, L.H. Li, A.G. Davies, E.H. Linfield, H.K. Liang, Y. Zhang, S.F. Yu, Q.J. Wang, Integrated terahertz graphene modulator with 100% modulation depth, ACS Photonics 2 (11) (2015) 1559–1566.
[79] Q. Li, Z. Tian, X. Zhang, R. Singh, L. Du, J. Gu, W. Zhang, Active graphene-silicon hybrid diode for terahertz waves, Nature Commun. 6 (2015) 7082.
[80] S. Arezoomandan, K. Yang, B. Sensale-Rodriguez, Graphene-based electrically reconfigurable deep-subwavelength metamaterials for active control of THz light propagation, Appl. Phys. A 117 (2) (2014) 423–426.
[81] S. Arezoomandan, B. Sensale-Rodriguez, Geometrical tradeoffs in graphene-based deeply-scaled electrically reconfigurable metasurfaces, Sci. Rep. 5 (2015) 8834.
[82] H.-T. Chen, W.J. Padilla, M.J. Cich, A.K. Azad, R.D. Averitt, A.J. Taylor, A metamaterial solid-state terahertz phase modulator, Nat. Photonics 3 (2009) 148.
[83] P.-Y. Chen, C. Argyropoulos, A. Alu, Terahertz antenna phase shifters using integrally-gated graphene transmission-lines, IEEE Trans. Antennas and Propagation 61 (4) (2013) 1528–1537.
[84] E. Carrasco, J. Perruisseau-Carrier, Reflectarray Antenna at Terahertz Using Graphene, IEEE Antennas Wireless Propagation Lett. 12 (2013) 253–256.
[85] H. Eisele, State of the art and future of electronic sources at terahertz frequencies, Electron. Lett. 46 (26) (2010) 8–11.

[86] H. Manohara, W.L. Dang, P.H. Siegel, M. Hoenk, A. Husain, A. Scherer, Field emission testing of carbon nanotubes for THz frequency vacuum microtube sources, in: Proc. SPIE 5343, Reliability, Testing, and Characterization of MEMS/MOEMS III, 227, 2004.
[87] S. Bhattacharjee, J.H. Booske, C.L. Kory, D.W. van der Weide, S. Limbach, S. Gallagher, J.D. Welter, M.R. Lopez, R.M. Gilgenbach, R.L. Ives, M.E. Read, R. Divan, D.C. Mancini, Folded waveguide traveling-wave tube sources for terahertz radiation, IEEE Trans. Plasma Sci. 32 (3) (2004) 1002–1014.
[88] T. Watanabe, T. Fukushima, Y. Yabe, S.A.B. Tombet, A. Satou, A.A. Dubinov, V.Y. Aleshkin, V. Mitin, V. Ryzhii, T. Otsuji, The gain enhancement effect of surface plasmon polaritons on terahertz stimulated emission in optically pumped monolayer graphene, New J. Phys. 15 (7) (2013) 075003.
[89] V. Ryzhii, M. Ryzhii, T. Otsuji, Negative dynamic conductivity in optically pumped graphene, J. Appl. Phys. 101 (2007) 083114.
[90] M. Ryzhii, V. Ryzhii, Injection and population inversion in electrically induced p–n junction in graphene with split gates, Japan. J. Appl. Phys. 46 (2) (2007) 8–11.
[91] V. Ryzhii, A.A. Dubinov, T. Otsuji, V. Mitin, M.S. Shur, Terahertz lasers based on optically pumped multiple graphene structures with slot-line and dielectric waveguides, J. Appl. Phys. 107 (2010) 054505.
[92] S. Boubanga-Tombet, S. Chan, T. Watanabe, A. Satou, V. Ryzhii, T. Otsuji, Ultrafast carrier dynamics and terahertz emission in optically pumped graphene at room temperature, Phys. Rev. B 85 (2012) 035443.
[93] T. Li, L. Luo, M. Hupalo, J. Zhang, M.C. Tringides, J. Schmalian, J. Wang, Femtosecond population inversion and stimulated emission of dense dirac fermions in graphene, Phys. Rev. Lett. 108 (2012) 167401.
[94] R.R. Nair, P. Blake, A.N. Grigorenko, K.S. Novoselov, T.J. Booth, T. Stauber, N.M.R. Peres, A.K. Geim, Fine structure constant defines visual transparency of graphene, Science 320 (5881) (2008) 1308.
[95] V. Ryzhii, M. Ryzhii, V. Mitin, T. Otsuji, Toward the creation of terahertz graphene injection laser, J. Appl. Phys. 110 (2011) 094503.
[96] L. Prechtel, L. Song, D. Schuh, P. Ajayan, W. Wegscheider, A.W. Holleitner, Time-resolved ultrafast photocurrents and terahertz generation in freely suspended graphene, Nature Commun. 3 (2012) 646.
[97] A. Tredicucci, M.S. Vitiello, Device concepts for graphene-based terahertz photonics, IEEE J. Sel. Top. Quantum Electron. 20 (2007) 8500109.
[98] F. Sizov, A. Rogalski, THz detectors, Prog. Quantum Electron. 34 (2010) 278–347.
[99] M.S. Vitiello, D. Coquillat, L. Viti, D. Ercolani, F. Teppe, A. Pitanti, F. Beltram, L. Sorba, W. Knap, A. Tredicucci, Room-temperature terahertz detectors based on semiconductor nanowire field-effect transistors, Nano Lett. 12 (2012) 96–101.
[100] A. Pitanti, D. Coquillat, D. Ercolani, L. Sorba, F. Teppe, W. Knap, G. De Simoni, F. Beltram, A. Tredicucci, M.S. Vitiello, Terahetz detection by heterostructed inas/insb nanowire based field effect transistors, Appl. Phys. Lett. 101 (2012) 141103.
[101] W. Knap, M. Dyakonov, D. Coquillat, F. Teppe, N. Dyakonova, J. Lausakowski, K. Karpierz, M. Sakowicz, G. Valusis, D. Seliuta, I. Kasalynas, A. El Fatimy, Y.M. Meziani, T. Otsuji, Field effect transistors for terahertz detection: Physics and first imaging applications, J. Infrared Millim. Terahertz Waves 30 (2009) 1319–1337.
[102] E. Ojefors, U.R. Pfeiffer, A. Lisauskas, H.G. Roskos, A 0.65 THz focal-plane array in a quarter-micron CMOS process technology, IEEE J. Solid-State Circuits 44 (2009) 1968–1976.
[103] M. Dyakonov, M. Shur, Shallow water analogy for a ballistic field effect transistor: new mechanism of plasma wave generation by dc current, Phys. Rev. Lett. 71 (1993) 2465–2468.
[104] M. Dyakonov, M. Shur, Choking of electron flow: A mechanism of current saturation in field-effect transistors, Phys. Rev. B 51 (1995) 14341–14345.
[105] M. Dyakonov, M. Shur, Detection, mixing, and frequency multiplication of terahertz radiation by two-dimensional electron fluid, IEEE Trans. Electron. Devices 43 (1996) 380–387.
[106] M. Dyakonov, M. Shur, Plasma wave electronics: novel terahertz devices using two dimensional electron fluid, IEEE Trans. Electron Devices 43 (1996) 1640–1645.
[107] W. Knap, V. Kachorovskii, Y. Deng, S. Rumyantsev, J.Q. Lu, R. Gaska, M.S. Shur, Nonresonant detection of terahertz radiation in field effect transistors, J. App. Phys. 91 (2002) 9346–9353.
[108] T. Otsuji, M. Hanabe, O. Ogawara, Terahertz plasma wave resonance of two-dimensional electrons in InGaP/InGaAs/GaAs high-electron mobility transistors, Appl. Phys. Lett. 85 (2004) 2119–2121.
[109] F. Teppe, W. Knap, D. Veksler, M.S. Shur, A.P. Dmitriev, V.Y. Kachorovskii, S. Rumyantsev, Room-temperature plasma waves resonant detection of sub-terahertz radiation by nanometer field effect transistor, Appl. Phys. Lett. 87 (2005) 052107.
[110] L. Vicarelli, M.S. Vitiello, D. Coquillat, A. Lombardo, A.C. Ferrari, W. Knap, M. Polini, V. Pellegrini, A. Tredicucci, Graphene field-effect transistors as room-temperature terahertz detectors, Nature Mater. 11 (2012) 865–871.
[111] A.H. Castro Neto, F. Guinea, N.M.R. Peres, K.S. Novoselov, A.K. Geim, The electronic properties of graphene, Rev. Modern Phys. 81 (2009) 109–162.
[112] A.N. Grigorenko, M. Polini, K.S. Novoselov, Graphene plasmonics, Nature Photon. 6 (2012) 749–758.
[113] M. Jablan, H. Buljan, M. Soljaccic, Plasmonics in graphene at infrared frequencies, Phys. Rev. B 80 (2009) 245435.
[114] R.M. Feenstra, D. Jena, G. Gu, Single-particle tunneling in doped graphene-insulator-graphene junctions, J. Appl. Phys. 111 (2012) 043711.
[115] V. Ryzhii, T. Otsuji, M. Ryzhii, M.S. Shur, Double graphene-layer plasma resonances terahertz detector, J. Phys. D: Appl. Phys. 45 (2012) 302001.
[116] V. Ryzhii, A. Satou, T. Otsuji, M. Ryzhii, V. Mitin, M.S. Shur, Dynamic effects in double graphene-layer structures with inter-layer resonant-tunnelling negative conductivity, J. Phys. D: Appl. Phys. 46 (2013) 315107.
[117] L. Britnell, R.V. Gorbachev, A.K. Geim, L.A. Ponomarenko, A. Mishchenko, M.T. Greenaway, T.M. Fromhold, K.S. Novoselov, L. Eaves, Resonant tunneling and negative differential conductance in graphene transistors, Nature Commun. 4 (2013) 1794-1-5.
[118] A. Mishchenko, J.S. Tu, Y. Cao, R.V. Gorbachev, J.R Wallbank, M.T. Greenaway, V.E. Morozov, S.V. Morozov, M.J. Zhu, S.L. Wong, F. Withers, C.R. Woods, Y.-J. Kim, K. Watanabe, T. Taniguchi, E.E. Vdovin, O. Makarovsky, T.M. Fromhold, V.I. Fal'ko, A.K. Geim, L. Eaves, K.S. Novoselov, Twist-controlled resonant tunnelling in graphene/boron nitride/graphene heterostructures, Nature Nanotechnol. 9 (2014) 808–813.
[119] B. Fallahazad, K. Lee, S. Kang, J. Xue, S. Larentis, C. Corbet, K. Kim, H.C.P. Movva, T. Taniguchi, K. Watanabe, L.F. Register, S.K. Banerjee, E. Tutuc, Gate-tunable resonant tunneling in double bilayer graphene heterostructures, Nano Lett. 15 (2014) 428–433.
[120] V. Ryzhii, T. Otsuji, V. Ya Aleshkin, A.A. Dubinov, M. Ryzhii, V. Mitin, M.S. Shur, Voltage-tunable terahertz and infrared photodetectors based on double-graphene-layer structures, Appl. Phys. Lett. 104 (2014) 163505.
[121] V. Ryzhii, T. Otsuji, M. Ryzhii, V. Mitin, M.S. Shur, Resonant plasmonic terahertz detection in vertical graphene-base hot-electron transistors, J. Appl. Phys. 118 (2015) 204501.
[122] A. Tomadin, A. Tredicucci, V. Pellegrini, M.S. Vitiello, M. Polini, Photocurrent-based detection of terahertz radiation in graphene, Appl. Phys. Lett. 103 (2013) 211120.
[123] V. Ryzhii, T. Otsuji, M. Ryzhii, V. Ya Aleshkin, A.A. Dubinov, D. Svintsov, V. Mitin, M.S. Shur, Graphene vertical cascade interband terahertz and infrared photodetectors, 2D Mater. 2 (2015) 025002.
[124] B. Sensale-Rodriguez, Graphene-insulator-graphene active plasmonic terahertz devices, Appl. Phys. Lett. 103 (2013) 123109.
[125] M. Ryzhii, V. Ryzhii, T. Otsuji, P.P. Maltsev, V.G. Leiman, N. Ryabova, V. Mitin, Double injection, resonant-tunneling recombination, and current–voltage characteristics in double-graphene-layer structures, J. Appl. Phys. 115 (2014) 024506.
[126] M. Hasan, B. Sensale-Rodriguez, Effect of the intra-layer potential distributions and spatial currents on the performance of graphene symfets, AIP Adv. 5 (2015) 097104.
[127] A. Zak, M.A. Andersson, M. Bauer, J. Matukas, A. Lisauskas, H.G. Roskos, J. Stake, Antenna-Integrated 0.6 THz FET direct detectors based on CVD graphene, Nano Lett. 14 (2014) 5834–5838.
[128] D. Spirito, D. Coquillat, S.L. De Bonis, A. Lombardo, M. Bruna, A.C. Ferrari, V. Pellegrini, A. Tredicucci, W. Knap, M.S. Vitiello, High performance bilayer-graphene terahertz detectors, Appl. Phys. Lett. 104 (2014) 061111.
[129] M. Mittendorff, S. Winnerl, J. Kamann, J. Eroms, D. Weiss, H. Schneider, M. Helm, Ultrafast graphene-based broadband THz detector, Appl. Phys. Lett. 103 (2013) 021113.
[130] M. Sakowicz, M.B. Lifshits, O.A. Klimenko, F. Schuster, D. Coquillat, F. Teppe, W. Knap, Terahertz responsivity of field effect transistors versus their static channel conductivity and loading effects, J. Appl. Phys. 110 (2011) 054512.
[131] W. Knap, S. Rumyantsev, M.S. Vitiello, D. Coquillat, S. Blin, N. Dyakonova, M. Shur, F. Teppe, A. Tredicucci, T. Nagatsuma, Nanometer size field effect transistors for terahertz detectors, Nanotechnology 24 (2013) 214002.
[132] N.M. Gabor, J.C.W. Song, Q. Ma, N.L. Nair, T. Taychatanapat, K. Watanabe, T. Taniguchi, L.S. Levitov, P. Jarillo-Herrero, Hotcarrier-assisted intrinsic photoresponse in graphene, Science 334 (2011) 648–652.
[133] J.C.W. Song, M.S. Rudner, C.M. Marcus, L.S. Levitov, Hot carrier transport and photocurrent response in graphene, Nano Lett. 11 (2011) 4688–4692.
[134] M. Freitag, T. Low, F. Xia, P. Avouris, Photoconductivity of biased graphene, Nat. Photonics 7 (2013) 53–59.
[135] Jun Yan, M.-H. Kim, J.A. Elle, A.B. Sushkov, G.S. Jenkins, H.M. Milchberg, M.S. Fuhrer, H.D. Drew, Dual-gated bilayer graphene hot-electron bolometer, Nature Nanotechnol. vol. 7 (2012) 472–478.
[136] M.-H. Kim, J. Yan, R.J. Suess, T.E. Murphy, M.S. Fuhrer, H.D. Drew, Photothermal response in dual-gated bilayer graphen, Phys. Rev. Lett. 110 (2013) 247402.
[137] X. Cai, A.B. Sushkov, R.J. Suess, M.M. Jadidi, G.S. Jenkins, L.O. Nyakiti, R.L. Myers-Ward, S. Li, J. Yan, D.K. Gaskill, T.E. Murphy, H.D. Drew, M.S. Fuhrer, Sensitive room-temperature terahertz detection via the photothermoelectric effect in graphene, Nature Nanotechnol. 9 (2014) 814–819.
[138] X. Cai, A.B. Sushkov, M.M. Jadidi, L.O. Nyakiti, Rachael L. Myers-Ward, D.K. Gaskill, T.E. Murphy, M.S. Fuhrer, H. Dennis Drew, Plasmon-Enhanced terahertz photodetection in graphene, Nano Lett. 15 (2015) 4295–4302.
[139] A.V. Muraviev, S.L. Rumyantsev, G. Liu, A.A. Balandin, W. Knap, M.S. Shur, Plasmonic and bolometric terahertz detection by graphene field-effect transistor, Appl. Phys. Lett. 103 (2013) 0181114.

Mehdi Hasan received the B.S. degree in Electrical and Electronic Engineering from Bangladesh University of Engineering and Technology, Dhaka, Bangladesh, in 2009, and the M.S. degree in Electrical and Computer Engineering from the University of New Mexico, Albuquerque, NM, USA, in 2012. He is currently pursuing the Ph.D. degree in Electrical and Computer Engineering at the University of Utah, Salt Lake City, UT, USA.

Sara Arezoomandan received the B.S. and M.S. degrees in Electrical Engineering from the University of Tehran, Tehran, Iran, in 2010 and 2013, respectively. She is currently pursuing the Ph.D. degree in Electrical and Computer Engineering at the University of Utah, Salt Lake City, UT, USA.

Hugo Condori received the B.S. degree in Electrical Engineering from Universidad Mayor de San Andres, La Paz, Bolivia, in 2010, and the M.S. degree in Electrical Engineering from Montana State University, Bozeman, MT, USA, in 2014. He is currently pursuing the Ph.D. degree in Electrical and Computer Engineering at the University of Utah, Salt Lake City, UT, USA.

Berardi Sensale-Rodriguez received the Engineer's degree from Universidad de la República, Montevideo, Uruguay, in 2008, and the Ph.D. degree in Electrical Engineering from the University of Notre Dame, Notre Dame, IN, USA, in 2013. He joined the faculty of the University of Utah, Salt Lake City, UT, USA, in 2013, where he is currently a tenure-track Assistant Professor of Electrical and Computer Engineering.